

A Mathematic Model on Differential Game based Flight-Path Angle Control Guidance Law

XING-YUAN XU^{1,2}, YUN-PENG LIANG², YUAN-LI CAI³

¹China Airborne Missile Academy, Luoyang, 471009, CHINA

²Information Engineering School, Henan University of Science and Technology,
Luoyang, 471023, CHINA

³Department of Automatic Control, Xi'an Jiao Tong University, Xi'an 710079, CHINA

Correspondence should be addressed to XING-YUAN XU; xuxingyuan2003@126.com

Abstract: - The increasing maneuverability potential of the target motivates designers to achieve high-performance guidance law. And, control of flight-path angle can increase interceptor (such as kinetic kill vehicle, KKV) lethality in the terminal engagement. The purpose of this manuscript is to achieve a differential game guidance law with a specified flight-path angle as well as zero terminal miss distance. In this manuscript, a pursuit-evasion differential game based guidance law is investigated for interceptors engaging against invasion aircraft, and the miss distance as well as the flight-path angle is treated as the performance index. Unlike previous work on this issue, the proposed guidance law suitable for intercepting high-speed maneuvering target, and, the proposed guidance law need not to know the target's future maneuver strategy. Numerical simulations are performed to investigate the performance of the proposed law.

Key-Words: - Differential game; flight-Path angle; guidance law; interceptor missile; mathematic model; maneuvering target.

1 Introduction

The primary objective of a guidance law is to guide a missile to its target point. In order to achieve this requirement, a missile needs the ability to adjust its flight path during flight via command acceleration. In addition to the main requirement, other requirements are also highly required, one such requirement might be to achieve a specified velocity direction relative to the target's velocity direction in the terminal engagement. This might be desirable, for example, kinetic kill vehicle (KKV) adopts the way of direct collision to destroy the target, therefore, a specific flight-path angle can ensure KKV to attack a weak spot on a target. The issue of flight-path angle control has been widely studied in the missile-guidance literature. Previous works on the problem of flight-path angle control were mainly focusing on a stationary or slowly moving target.

The most widely known and used guidance law is proportional navigation guidance (PNG) law and its various variants, because of its inherent simplicity and ease of implementation [1,2]. PNG seeks to null the line-of-sight (LOS) rate against nonmaneuvering targets by making the interceptor missile heading proportional to the LOS rate. Traditional PNG laws are designed primarily for minimizing the miss distance, and they are usually silent on flight-path angle constraints. However, within the PN philosophy, some variations like time-varying gains,

bias terms, etc., have been proposed in the recent literature to cater for flight-path angle constraint as well [3-5]. In [4], a modified PNG with a time-varying bias (BPNG) was proposed, the time-varying bias is an intuitive function of state variables such as LOS angle, relative range, and flight-path angle. The capture zone of the proposed guidance law was computed by studying a Lyapunov-like function. Ref. [5] proposed a bias-shaping based two-phase BPNG, which follows BPNG with a constant bias for the initial homing phase and then switches to PNG (i.e., BPNG with zero bias) when the integral value of the bias satisfies a certain value calculated from initial engagement conditions and desired flight-path angle. Because the two-phase guidance schemes only use the LOS rate information for the flight-path angle control, it can be applied to passive homing missile systems. A similar approach using bias-shaping method BPNG law was suggested to satisfy the same principle [6]. Lu et al. [7] have used PNG in an adaptive guidance law for a hypervelocity flight-path angle constrained hit at a stationary target. Satisfying flight-path angle constraint by varying the navigation constant N of the PNG is addressed by Ratnoo and Ghose [8]. In their work, a two-stage PNG law is proposed for achieving all flight-path angles against stationary targets in surface-to-surface engagements.

During the past several years, optimal control theory [9-11] has been successfully applied to solve flight-path angle control problems by considering control energy. This approach can obtain a single form of guidance law that achieves the desired flight-path angle. For optimal guidance with flight-path angle control, the optimal guidance law is given by solving the linear quadratic optimal control problem. Ryoo et al. [12] proposed a generalized formulation of the energy minimization optimal guidance problem for a constant speed missile with an arbitrary system to achieve the desired flight-path angle as well as the desired zero miss distance. They also proposed a time-to-go weighted optimal guidance law that was obtained by the solution of a linear quadratic optimal control problem with the energy cost weighted by a power of the time-to-go [13]. Ratnoo et al. [8] proposed a state-dependent Riccati equation technique to achieve the desired flight-path angle. Among the methods other than linear quadratic theory in the 2-D category is the flight-path angle constrained guidance law using orientation geometry as proposed by Ref. [14]. Lee et al. [9] demonstrated optimality of linear time-varying guidance laws for flight-path angle control using inverse optimal control theory.

Although various guidance laws to control the flight-path angle have a good homing accuracy against non-maneuvering targets, recent simulation studies indicated that they are unable to guarantee an adequate homing accuracy in the interception of the highly maneuvering target. The reason is that future target's maneuver strategy cannot be predicted, however, the majority of currently used guidance laws, such as optimal guidance laws (OGL), rely on exact knowledge of the target dynamics. The mathematical framework for analyzing conflicts controlled by two independent agents is in the realm of dynamic games. Thus, the scenario of intercepting a maneuverable target has to be formulated as a zero-sum pursuit-evasion game. The roles of the players are clearly defined, the interceptor is the pursuer and the target is the evader [15]. Two differential game based guidance laws were proposed in Ref. [15], however, the cost function includes the miss distance component but not flight-path angle, the pursuer's guidance law is obtained through minimizing the miss distance and the evader's guidance law is obtained through maximizing the miss distance.

The majority of the guidance laws with control of terminal flight-path angle reviewed above are only suitable for stationary or slowly moving target. The aim of this research is to obtain an explicit-form linear quadratic differential game (LQDG) guidance

law, which can achieve the desired flight-path angle as well as zero miss distance. The specific objectives are: to present the formulation of the LQDG guidance law, to discuss the influence of the parameters in the guidance law, and to carry out nonlinear simulations to validate the proposed guidance law.

2 Problem Formulation

The engagement between two missiles—a pursuer (interceptor) and an evader (target)—is considered. Considering only a planar engagement can not represent a drawback either in theory, or for applications. It has been demonstrated by Adler that if the trajectory linearization is valid, the three-dimensional equations can be decoupled into two identical planar sets [16]. In practice, the great majority of guided missiles have cruciform configurations and two identical guidance channels operating in perpendicular planes.

In Fig.1, a schematic view of interception geometry is shown. The X-axis of the coordinate system is aligned with the initial LOS. The pursuer is denoted as P and the evader is denoted as E. V_P , V_E are the constant speeds of the pursuer and evader, respectively; a_P , a_E are the lateral accelerations of the pursuer and evader, respectively; The flight-path angles of the pursuer and evader are denoted by γ_P , γ_E , respectively; The relative range between the adversaries is R , and θ is the angle between the LOS and X-axis. The relative displacement between adversaries normal to the initial LOS is y . The pursuer and evader accelerations normal to the initial LOS are denoted by a_{PN} and a_{EN} , respectively; And satisfy $a_{PN} = a_P \cos \gamma_{P0}$, $a_{EN} = a_E \cos \gamma_{E0}$. The required flight-path angle is equal to $\gamma_P + \gamma_E$.

From the engagement geometry of Fig.1, the range between the pursuer and the evader has a value R , and the LOS has rotated through an angle

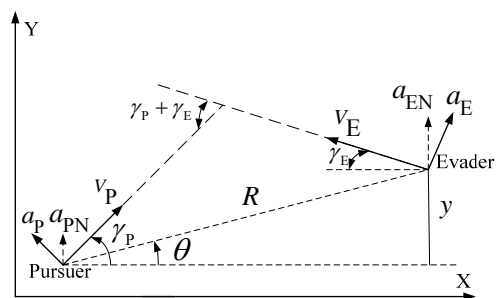


Fig.1 Geometry for derivation of the LQDG guidance law

θ from the initial value. The rate of rotation of the LOS at any time is given by the difference in the normal components of velocity of the pursuer and evader, divided by the range. This can be expressed by the equation

$$\dot{\theta} = \frac{-V_p \sin(\gamma_p - \theta) + V_E \sin(\gamma_E + \theta)}{R} \quad (1)$$

The velocity component along the LOS is given by the equation

$$\dot{R} = -V_p \cos(\gamma_p - \theta) - V_E \cos(\gamma_E + \theta) \quad (2)$$

During the endgame, the pursuer and evader are assumed to move at a constant speed. In addition, assuming the evader has a first-order lateral maneuver dynamics. Thus,

$$\dot{a}_E = \frac{u_E - a_E}{\tau_E} \quad (3)$$

$$\dot{\gamma}_E = a_E / V_E \quad (4)$$

where u_E is the evader's command acceleration and τ_E is the evader's time constant.

Suppose the pursuer is a lag-free system, such as KKV, thrusters provide the normal acceleration directly and the response of the propulsion system is rapid enough, the system delay can be ignored [17]. In this case

$$a_p = u_p \quad (5)$$

where u_p is the pursuer's command acceleration.

$$\dot{\gamma}_p = a_p / V_p \quad (6)$$

If non-zero-lag dynamics were assumed for the pursuer, the processing method is similar. The assumption of lag-free dynamics is only due to the simplicity and ease of presentation. In order to well illustrate the LQDG guidance law, this treatment method is reasonable.

All the above assumptions lead to the following linear model for $t_0 \leq t \leq t_f$

$$\begin{cases} \dot{x}_1 = x_2 \\ \dot{x}_2 = a_E \cos \gamma_{E0} - a_p \cos \gamma_{p0} \\ \dot{x}_3 = \frac{u_E - a_E}{\tau_E} \\ \dot{x}_4 = a_E / V_E + a_p / V_p \end{cases} \quad (7)$$

where $x_1 = y$ is the difference between the evader's and pursuer's position normal to the initial LOS; x_2 is the relative lateral velocity; x_3 is the lateral acceleration of the evader; and x_4 is the required flight-path angle ($\gamma_p + \gamma_E$).

Consider now the linear dynamical system characterized by the canonical equation

$$\dot{\mathbf{x}} = \mathbf{A}\mathbf{x} + \mathbf{B}\mathbf{u}_p + \mathbf{C}\mathbf{u}_E \quad (8)$$

From Eqs.(3-8), one can obtain

$$\mathbf{A} = \begin{bmatrix} 0 & 1 & 0 & 0 \\ 0 & 0 & \cos \gamma_{E0} & 0 \\ 0 & 0 & -1/\tau_E & 0 \\ 0 & 0 & 1/V_E & 0 \end{bmatrix}, \mathbf{B} = \begin{bmatrix} 0 \\ -\cos \gamma_{p0} \\ 0 \\ 1/V_p \end{bmatrix}, \mathbf{C} = \begin{bmatrix} 0 \\ 0 \\ 1/\tau_E \\ 0 \end{bmatrix}$$

$$\mathbf{x} = (\mathbf{x}_1, \mathbf{x}_2, \mathbf{x}_3, \mathbf{x}_4)^T \quad (9)$$

If the pursuer and evader deviations from the collision triangle are small in the terminal engagement, that is, the endgame is initiated with a collision triangle satisfying closely the requirement on the flight-path angle ($\gamma_p + \gamma_E$), this initialization can be performed by a nonlinear midcourse guidance law. Then, the collision triangle is maintained, the closing velocity between pursuer and evader is constant and the total time of flight can be assumed fixed. The time-to-go can be estimated as follow

$$t_g = -\frac{R}{\dot{R}} \quad (11)$$

3 Linear Quadratic Differential Games Guidance Law

Compare with other guidance laws, in the derivation of the LQDG guidance law, target maneuvers are independently controlled and they cannot be predicted. The mathematical framework for analyzing conflicts controlled by two independent agents is in the realm of dynamic games. Thus, the scenario of intercepting a maneuverable target has to be formulated as a zero-sum game. The performance index to be minimized will be assumed to be given by

$$J = \frac{1}{2} \mathbf{e}(t_f)^T \mathbf{S} \mathbf{e}(t_f) + \frac{1}{2} \int_0^{t_f} [\mathbf{u}_p(\tau) - \mu^2 \mathbf{u}_E(\tau)] d\tau \quad (12)$$

where $\mathbf{e}(t_f) = \mathbf{x}(t_f) - \mathbf{x}_f$ is terminal states error at the intercept time t_f and \mathbf{x}_f is the desired terminal state. The term $\mathbf{e}(t_f)^T \mathbf{S} \mathbf{e}(t_f)$ is a penalty for deviations from the terminal state. The pursuer control signal $\mathbf{u}_p(t)$ is obtained through minimizing J , which discourages the pursuer from use of large control effort. The evader control signal $\mathbf{u}_E(t)$ is obtained through maximizing J , which encourages the evader from use of large control effort. Here, $\mathbf{S} \geq 0$ (semi-positive definite), and \mathbf{S} is the final

state error weighting matrix. μ represents the evader's maneuvering capability relative to that of the pursuer, and μ is selected by the guidance analyst. There are four state vector in (7), however, the guidance law in this work only emphasize x_1 and x_4 , that is, miss distance and flight-path angle. Thus, the system (7) can be reduced to a 2×1 vector using the transformation

$$Z(t) = \mathbf{D}\Phi(t_f, t)\mathbf{x}(t) \quad (13)$$

Here, $\Phi(t_f, t)$ denotes the state transition matrix to propagate the state from t_0 to t_f , and \mathbf{D} is a constant matrix

$$\mathbf{D} = \begin{bmatrix} 1 & 0 & 0 & 0 \\ 0 & 0 & 0 & 1 \end{bmatrix} \quad (14)$$

The 2×1 vector variable $Z(t)$ represents the zero-effort miss and zero-effort flight-path angle. Then, the derivative with respect to time of the new state vector $Z(t)$ is

$$\dot{Z}(t) = \mathbf{D}\Phi(t_f, t)\mathbf{B}\mathbf{u}_p(t) + \mathbf{D}\Phi(t_f, t)\mathbf{C}\mathbf{u}_E(t) \quad (15)$$

where

$$\Phi(t_f, t) = \begin{bmatrix} 1 & t_f - t & (-\tau_E^2 + \tau_E(t_f - t) + \tau_E^2 e^{\frac{t_f - t}{\tau_E}}) \cos \gamma_{E0} & 0 \\ 0 & 1 & (\tau_E - \tau_E e^{\frac{t_f - t}{\tau_E}}) \cos \gamma_{E0} & 0 \\ 0 & 0 & e^{\frac{t_f - t}{\tau_E}} & 0 \\ 0 & 0 & \frac{(\tau_E - \tau_E e^{\frac{t_f - t}{\tau_E}})}{V_E} & 1 \end{bmatrix} \quad (16)$$

The proof of (15) is shown in the appendix.

$Z(t_f)$ can be expressed as

$$\mathbf{Z}(t_f) = \mathbf{D}\Phi(t_f, t)\mathbf{x}(t) = \mathbf{D}\mathbf{x}(t_f) = \begin{bmatrix} x_1(t_f) \\ x_4(t_f) \end{bmatrix} \quad (17)$$

Using the new state vector $Z(t)$, and, selecting the following weight

$$\mathbf{S} = \begin{bmatrix} a_1 & 0 \\ 0 & a_2 \end{bmatrix} \quad (18)$$

where a_1, a_2 are nonnegative coefficients, and a_1, a_2 are selected by the guidance analyst. Defining $\gamma_f = \gamma_p + \gamma_E$, the cost function from Eq. (12) can also be expressed as

$$J = \frac{a_1}{2} Z_1^2(t_f) + \frac{a_2}{2} [Z_2(t_f) - \gamma_f]^2 + \frac{1}{2} \int_0^{t_f} (u_p^2 - \mu^2 u_E^2) dt \quad (19)$$

The zero-effort miss and flight-path angle varies in accordance with the following equation

$$\dot{Z}(t) = \begin{bmatrix} -t_g \cos \gamma_{p0} \\ 1/V_p \end{bmatrix} \mathbf{u}_p + \begin{bmatrix} (-\tau_E + t_g + \tau_E e^{\frac{t_g}{\tau_E}}) \cos \gamma_{E0} \\ \frac{(1 - e^{\frac{t_g}{\tau_E}})}{V_E} \end{bmatrix} \mathbf{u}_E \quad (20)$$

In order to well illustrate the LQDG law, ideal dynamics of the evader is considered, i.e., $\tau_E = 0$. In this case,

$$\dot{Z}(t) = \begin{bmatrix} -t_g \cos \gamma_{p0} \\ 1/V_p \end{bmatrix} \mathbf{u}_p + \begin{bmatrix} t_g \cos \gamma_{E0} \\ \frac{1}{V_E} \end{bmatrix} \mathbf{u}_E \quad (21)$$

The projection of the adversary's command acceleration in the direction perpendicular to the initial LOS are $u = u_p \cos \gamma_{p0}$, $v = u_E \cos \gamma_{E0}$, respectively. The adversary's velocity components on the initial LOS are $V_p' = V_p \cos \gamma_{p0}$, $V_E' = V_E \cos \gamma_{E0}$, respectively. Then, Eq.(21) simplified to

$$\begin{cases} \dot{Z}_1 = -t_g u + t_g v \\ \dot{Z}_2 = u/V_p' + v/V_E' \end{cases} \quad (22)$$

According to Eqs.(19) and (22), one can obtain the following optimal controller

$$\begin{cases} \mathbf{u}^*(t) = \frac{\mathbf{A}_1}{t_g^2} Z_1(t) + \mathbf{A}_2 \frac{\mathbf{V}_p'}{t_g} [Z_2(t) - \gamma_f] \\ \mathbf{v}^*(t) = \frac{\mathbf{B}_1}{t_g^2} Z_1(t) + \mathbf{B}_2 \frac{\mathbf{V}_p'}{t_g} [Z_2(t) - \gamma_f] \end{cases} \quad (23)$$

Where

$$\mathbf{A}_1 = \frac{3a_1 \mu^2 t_g^3}{\Delta} + \frac{a_2 \mathbf{W}_2(t_g) t_g^2}{\mathbf{W}_1(t_g)} \left(\frac{3a_1 \mu^2 \mathbf{V}_1 t_g^3}{2\Delta} - \frac{1}{V_p'} \right) \quad (24)$$

$$\mathbf{A}_2 = \frac{a_2 t_g}{\mathbf{V}_p' \mathbf{W}_1(t_g)} \left(\frac{3a_1 \mu^2 \mathbf{V}_1 t_g^3}{2\Delta} - \frac{1}{V_p'} \right) \quad (25)$$

$$\mathbf{B}_1 = \frac{1}{\mu^2} \left[\frac{3a_1 \mu^2 t_g^3}{\Delta} + \frac{a_2 \mathbf{W}_2(t_g) t_g^2}{\mathbf{W}_1(t_g)} \left(\frac{3a_1 \mu^2 \mathbf{V}_1 t_g^3}{2\Delta} + \frac{1}{V_E'} \right) \right] \quad (26)$$

$$\mathbf{B}_2 = \frac{a_2 t_g}{\mu^2 \mathbf{V}_p' \mathbf{W}_1(t_g)} \left(\frac{3a_1 \mu^2 \mathbf{V}_1 t_g^3}{2\Delta} + \frac{1}{V_E'} \right) \quad (27)$$

$$\mathbf{V}_1 = \frac{\mathbf{V}_E' \mu^2 + \mathbf{V}_p'}{\mathbf{V}_p' \mathbf{V}_E' \mu^2} \quad (28)$$

$$\mathbf{V}_2 = \frac{\mathbf{V}_p'^2 - \mu^2 \mathbf{V}_E'^2}{\mathbf{V}_p'^2 \mathbf{V}_E'^2 \mu^2} \quad (29)$$

$$\Delta = 3\mu^2 - (1 - \mu^2) a_1 t_g^3 \quad (30)$$

$$\mathbf{W}_1(t_g) = 1 - a_2 \mathbf{V}_2 t_g - \frac{3a_1 a_2 \mu^2 \mathbf{V}_1^2 t_g^4}{4\Delta} \quad (31)$$

$$\mathbf{W}_2(t_g) = \frac{3a_1 \mu^2 \mathbf{V}_1 t_g^2}{2\Delta} \quad (32)$$

The proof of Eqs. (23-32) is shown in the appendix. As mentioned above, through the new state vector

$\mathbf{Z}(t)$, the order of the problem is reduced. In addition, the two variables of $\mathbf{Z}(t)$ have other important physical meaning. $Z_1(t)$ is known as the zero-effort miss, which, in a two-sided optimization problem, is the miss distance if, from the current time onward, both the pursuer and the evader will not apply any controls. $Z_2(t)$ is known as zero-effort angle, which, is the flight-path angle if, from the current time onward, both the pursuer and the evader will not apply any controls. Then, $Z_2(t) - \gamma_f$ can be denoted as the zero-effort angle error. $Z_1(t)$ and $Z_2(t)$ can be expressed as

$$Z_1(t) = y + \dot{y}t_g \tag{33}$$

$$Z_2(t) = \gamma_E + \gamma_P \tag{34}$$

For the implementation of the guidance law which is given by Eqs. (23-32), the pursuer requires a built-in inertial navigation system (INS) to obtain the necessary information, such as $Z_1(t)$, $Z_2(t)$, t_g , V_p' . Under the assumption of small LOS angle, and the pursuer can measure the LOS angle $\theta(t)$, the relative displacement y can be approximated by

$$y \approx \theta R \tag{35}$$

Then, equation (33) can be expressed as

$$Z_1(t) = y + \dot{y}t_g = -\dot{\theta}Rt_g^2 \tag{36}$$

Here, V_p' , γ_P and \dot{R} can be directly measured by INS, $\dot{\theta}$ can be measured by an additional seeker, γ_E , α_E , V_E and t_g can be estimated through corresponding formulas.

4 Numerical Analysis

The performance of the proposed LQDG guidance law is investigated in this section through numerical simulations. The initial condition for the non-linear simulations is given in Table 1.

Fig. 2 presents trajectories of pursuer and evader for various flight-path angles; Figs. 3 and 4 denote optimal guidance commands of pursuer and evader

Parameter	value
Pursuer initial position	(0 m, 0 m)
Evader initial position	(0 m, 10000 m)
Pursuer flight velocity	1500 m/s
Evader flight velocity	1500 m/s
Pursuer initial flight path angle	0°
Evader initial flight path angle	0°

Parameter μ	9
Constant coefficient a_1	10^5
Constant coefficient a_2	10^8

for various flight-path angles corresponding to Fig.2, respectively. From Fig.3, the guidance commands for various flight-path angles are not large near the terminal time, this is a great advantage of the proposed guidance law. Also, one can see from Fig.3, the larger the required interceptor angle, the greater the magnitude of the maximal control command, this is due to large angle correction required. And, the maximal command acceleration increases when μ decreases. Thus, in order to avoid command saturation, the value of μ should not too small. The change trends of zero-effort miss $Z_1(t)$ and zero-effort flight-path angles $Z_2(t)$ are shown in Figs. 5 and 6. One can see, zero-effort miss tend to zero, and zero-effort interceptor angles tend to the desired flight-path angles. Navigation gains A_1 , A_2 , B_1 and B_2 are bound up with the values of a_1 , a_2 and μ . Figs. 7-10 show the change trends of A_1 , A_2 , B_1 and B_2 with a_2 , respectively. Fig. 11 shows change trends of A_1 , A_2 , B_1 and B_2 with μ for perfect intercept (zero miss distance) and perfect intercept angle(zero intercept angle error). We will go into details of the influence of the parameters A_1 , A_2 , B_1 , B_2 and μ in section 5.

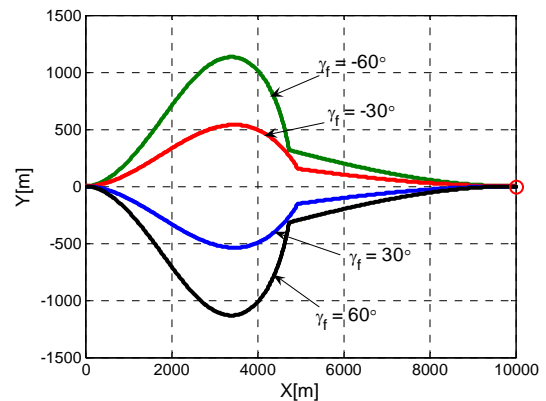


Fig.2 Optimal trajectories of pursuer and evader for various flight-path angles

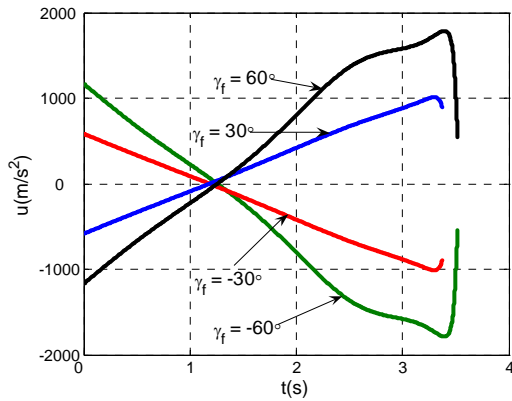


Fig.3 Optimal guidance commands of pursuer for various flight-path angles

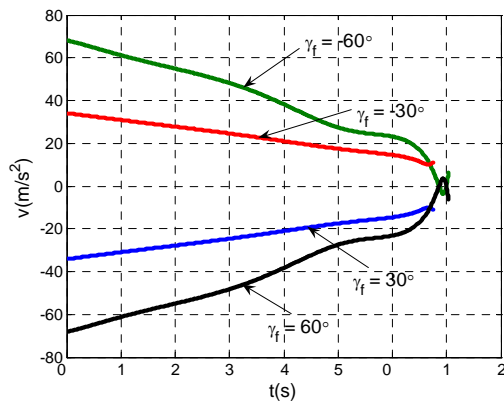


Fig.4 Optimal guidance commands of evader for various flight-path angles

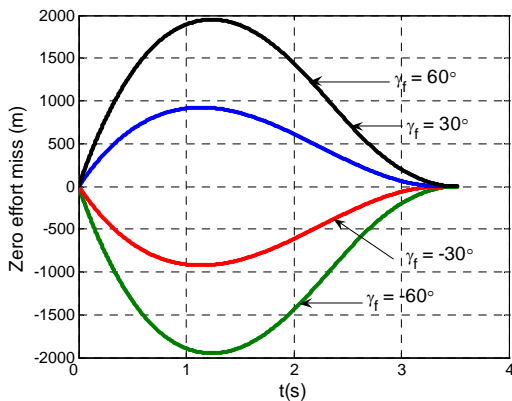


Fig.5 Histories of the zero-effort miss $Z_1(t)$

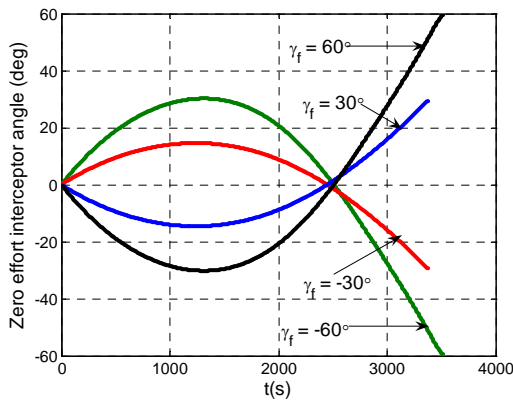


Fig.6 Histories of the zero-effort interceptor angles $Z_2(t)$

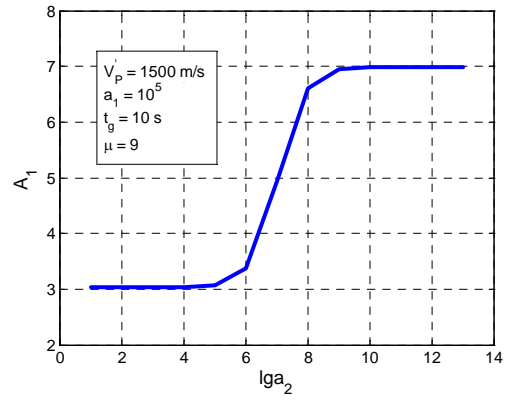


Fig.7 Change trends of A_1 vs $\lg a_2$

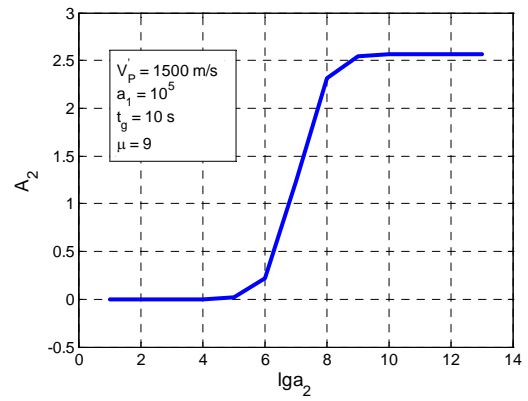


Fig.8 Change trends of A_2 vs $\lg a_2$

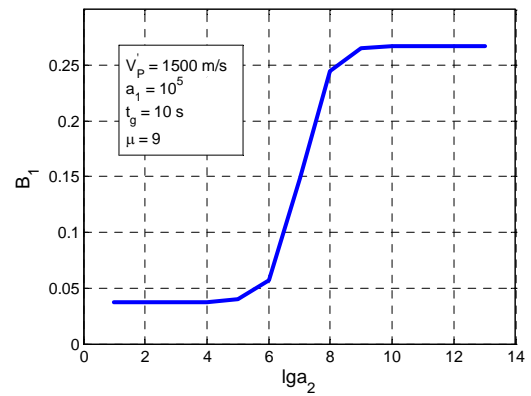


Fig.9 Change trends of B_1 vs $\lg a_2$

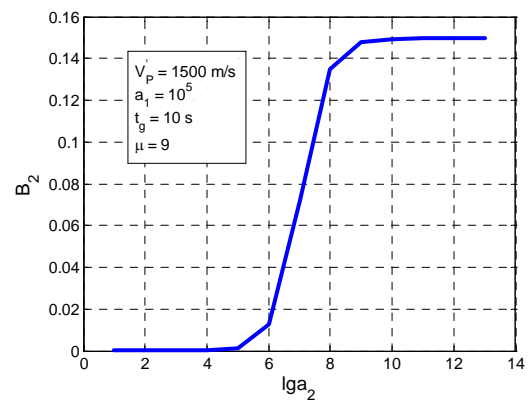


Fig.10 Change trends of B_2 vs $\lg a_2$

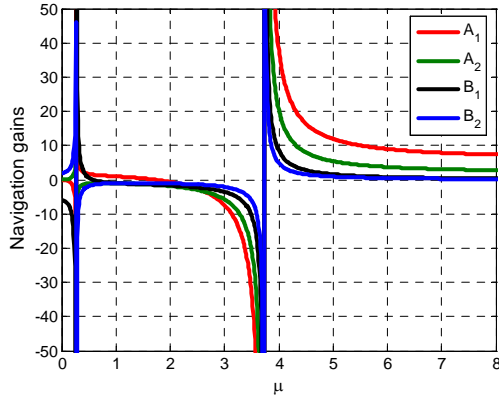


Fig.11 Change trends of navigation gains vs μ for perfect intercept and intercept angle

5 Discussion

As mentioned above, the magnitude of a_1 , a_2 and μ are to exercise a great influence on the proposed guidance law. In this section, a critical evaluation of the proposed LQDG guidance law will be presented.

5.1 Influence of a_1 and a_2

As shown in Eq. (23), the first term is responsible for zero the miss distance, i.e., intercepting the evader. The second term is responsible for zero the interceptor angle error, i.e., achieving a desired flight-path angle. By choosing $a_2 \rightarrow 0$, the proposed LQDG guidance law degenerate to the LQDG guidance law presented in [18], i.e., no longer impose an flight-path angle. In this case, the navigation gains are

$$\begin{cases} \lim_{a_2 \rightarrow 0} A_1 = \frac{3\mu^2 a_1 t_g^3}{3\mu^2 - (1 - \mu^2) a_1 t_g^3} \\ \lim_{a_2 \rightarrow 0} A_2 = 0 \\ \lim_{a_2 \rightarrow 0} B_1 = \frac{3a_1 t_g^3}{3\mu^2 - (1 - \mu^2) a_1 t_g^3} \\ \lim_{a_2 \rightarrow 0} B_2 = 0 \end{cases} \quad (37)$$

Also, choosing $a_1 \rightarrow \infty$ and $\mu \rightarrow \infty$, the guidance law further degenerates to the well-known optimal PN guidance law presented in [18], which is only suitable for nonmaneuvering target and the navigation gain A_1 is 3.

$$\begin{cases} \lim_{\substack{a_1 \rightarrow \infty \\ a_2 \rightarrow 0 \\ \mu \rightarrow \infty}} A_1 = 3 \\ \lim_{\substack{a_1 \rightarrow \infty \\ a_2 \rightarrow 0 \\ \mu \rightarrow \infty}} A_2 = 0 \\ \lim_{\substack{a_1 \rightarrow \infty \\ a_2 \rightarrow 0 \\ \mu \rightarrow \infty}} B_1 = 0 \\ \lim_{\substack{a_1 \rightarrow \infty \\ a_2 \rightarrow 0 \\ \mu \rightarrow \infty}} B_2 = 0 \end{cases} \quad (38)$$

For achieving a perfect intercept (zero miss distance) with some account for flight-path angle, $a_1 \rightarrow \infty$ and a finite a_2 are required, in this case

$$\begin{cases} \lim_{a_1 \rightarrow \infty} A_1 = \frac{3\mu^2}{\mu^2 - 1} + \frac{6\mu^2 a_2 V_1 t_g}{\Delta} \left(\frac{3\mu^2 V_1}{2(1 - \mu^2)} + \frac{1}{V_p'} \right) \\ \lim_{a_1 \rightarrow \infty} A_2 = \frac{4a_2 (\mu^2 - 1) t_g}{V_p' \Delta} \left(\frac{3\mu^2 V_1}{2(1 - \mu^2)} + \frac{1}{V_p'} \right) \\ \lim_{a_1 \rightarrow \infty} B_1 = \frac{3}{\mu^2 - 1} + \frac{6a_2 V_1 t_g}{\Delta} \left(\frac{3\mu^2 V_1}{2(1 - \mu^2)} - \frac{1}{V_E'} \right) \\ \lim_{a_1 \rightarrow \infty} B_2 = \frac{4a_2 (\mu^2 - 1) t_g}{V_p' \mu^2 \Delta} \left(\frac{3\mu^2 V_1}{2(1 - \mu^2)} - \frac{1}{V_E'} \right) \end{cases} \quad (39)$$

where

$$\Delta = 4(1 - \mu^2) + a_2 t_g [3\mu^2 V_1^2 - 4(1 - \mu^2) V_2] \quad (40)$$

By choosing $a_1 \rightarrow \infty$ and $a_2 \rightarrow \infty$, a perfect intercept and perfect interceptor angle will be achieved, in this case,

$$\begin{cases} \lim_{\substack{a_1 \rightarrow \infty \\ a_2 \rightarrow \infty}} A_1 = \frac{6\mu^2}{\Delta_\infty} \left(2V_2 + \frac{V_1}{V_p'} \right) \\ \lim_{\substack{a_1 \rightarrow \infty \\ a_2 \rightarrow \infty}} A_2 = \frac{1}{V_p' \Delta_\infty} [6\mu^2 V_1 V_p' + 4(1 - \mu^2)] \\ \lim_{\substack{a_1 \rightarrow \infty \\ a_2 \rightarrow \infty}} B_1 = \frac{6}{\Delta_\infty} \left(2V_2 - \frac{V_1}{V_E'} \right) \\ \lim_{\substack{a_1 \rightarrow \infty \\ a_2 \rightarrow \infty}} B_2 = \frac{1}{\mu^2 V_p' V_E' \Delta_\infty} [6\mu^2 V_1 V_E' - 4(1 - \mu^2)] \end{cases} \quad (41)$$

where

$$\Delta_\infty = 3\mu^2 V_1^2 - 4(1 - \mu^2) V_2] \quad (42)$$

Figs. 7-10 presents the change trends of the navigation gains A_1 , A_2 , B_1 and B_2 with a_2 , respectively. Note that the navigation gains A_1 , A_2 , B_1 and B_2 are not a function of t_g for $a_1 \rightarrow \infty$ and $a_2 \rightarrow \infty$.

5.2 Influence of μ

The constant μ presents maneuvering capability of the evader compared with the pursuer. Thus, a smaller μ (a more maneuverable evader) means

larger navigation gains are obtained. If the evader is nonmaneuvering, a large value of μ should be chosen and vice versa.

As mentioned above, LQDG guidance law can guarantee perfect intercept and perfect intercept angle by choosing $a_1 \rightarrow \infty$ and $a_2 \rightarrow \infty$. Thus, The navigation gains are unbounded when $\Delta_\infty \rightarrow 0$, in this case, the gains diverge and the guidance law is no longer optimal. The critical value of μ is denoted as μ_c , and μ_c can be solved from $\Delta_\infty \rightarrow 0$. From Fig. 11, one can see, navigation gains diverge when $\mu = \mu_c$. The influence of μ is a very complicated subject, this work will not discuss the issue in detail. In general, $|\mu| > \mu_c$ should be selected.

For a perfect intercept and perfect interceptor angle point to a nonmaneuvering evader ($\mu \rightarrow \infty$), the navigation gains further degenerate to

$$\left\{ \begin{array}{l} \lim_{\substack{a_1 \rightarrow \infty \\ a_2 \rightarrow \infty \\ \mu \rightarrow \infty}} \mathbf{A}_1 = 6 \\ \lim_{\substack{a_1 \rightarrow \infty \\ a_2 \rightarrow \infty \\ \mu \rightarrow \infty}} \mathbf{A}_2 = 2 \\ \lim_{\substack{a_1 \rightarrow \infty \\ a_2 \rightarrow \infty \\ \mu \rightarrow \infty}} \mathbf{B}_1 = 0 \\ \lim_{\substack{a_1 \rightarrow \infty \\ a_2 \rightarrow \infty \\ \mu \rightarrow \infty}} \mathbf{B}_2 = 0 \end{array} \right. \quad (43)$$

Substituting Eq. (43) into Eq. (23), one can obtain

$$\left\{ \begin{array}{l} \mathbf{u}^*(t) = \frac{6}{t_g^2} \mathbf{Z}_1(t) + 2 \frac{\mathbf{V}_p'}{t_g} [\mathbf{Z}_2(t) - \gamma_f] \\ \mathbf{v}^*(t) = 0 \end{array} \right. \quad (44)$$

From Eq. (44), one can see, the evader's guidance commands are nulled and the pursuer's guidance law is similar to the optimal PN cases. Moreover, the gain associated with the zero-effort miss is multiplied by a factor of 2 compared with the optimal PN cases, which might result in an increased sensitivity to measurement noise [19].

4 Conclusion

In this manuscript, a linear quadratic differential game guidance law which enables imposing a specified flight-path angle has been derived. The LQDG guidance law is best suited when the target maneuver is unknown. The roles of the players are clearly defined, the interceptor is the pursuer and the target is the evader. The cost function of such zero-sum game is the miss distance and flight-path angle

error, to be minimized by the pursuer and maximized by the evader. The game solution provides simultaneously the pursuer's guidance law (the optimal pursuer strategy), the "worst" target maneuver (the optimal evader strategy). Simulation results show that the proposed LQDG guidance law produces good performance. And, the guidance commands are not large near the terminal time, which is an advantage compared with the majority of similar work on the issue. The navigation gains of the closed-form solutions were studied, and their behavior was analyzed for the perfect intercept and perfect intercept angle case. In application of the proposed guidance law, information such as the current position, LOS angle, and velocity can be provided by a built-in inertial navigation system and a normal seeker.

References:

- [1] Zarchan P, *Tactical and strategic missile guidance, fifth edition (Progress in Astronautics and Aeronautics)*, AIAA, 5th ed., 2007.
- [2] Siouris GM, *Missile Guidance and Control Systems*, Springer, New York, 2003.
- [3] Oza HB and Padhi R, Impact-angle-constrained suboptimal model predictive static programming guidance of air-to-ground missiles, *J Guidance Cont Dynam*, Vol.35, No.1, 2012, pp. 153–164.
- [4] Kim BS, Lee JG and Han SH, Biased PNG law for impact with angular constraint, *IEEE Trans Aerosp Electron Syst*, Vol.34, No.1, 1998, pp. 277–288.
- [5] Ezer KS and Merttopçuo LO, Indirect impact-angle-control against stationary targets using biased pure proportional navigation, *J Guidance Cont Dynam*, Vol.35, No.2, 2012, pp. 700–703.
- [6] Kim TH, Park BG and Tahk MJ, Bias-shaping method for biased proportional navigation with terminal-angle constraint, *J Guidance Cont Dynam*; Ahead of print: 1–6.
- [7] Lu P, Doman DB and Schierman JD, Adaptive terminal guidance for hypervelocity impact in specified direction, *J Guidance Cont Dynam*, Vol.29, No.2, 2006, pp. 269–278.
- [8] Ratnoo A and Ghose D, Impact angle constrained interception of stationary targets, *J Guidance Cont Dynam*, Vol.31, No.6, 2008, pp. 1816–1821.

[9] Lee YI, Kim SH and Tahk MJ, Optimality of linear time-varying guidance for impact angle control, *IEEE Trans Aerosp Electron Syst*, Vol.48, No.4, 2012, pp. 2802–2817.

[10] Dwivedi PN, Bhattacharya A and Padhi R, Computationally efficient suboptimal midcourse guidance using model predictive static programming, *In: Proceedings of IFAC World Congress*, Seoul, ROK, 6-11 July 2008, pp.3550-3555.

[11] Tatiya M, Bhatia N and Padhi R, Impact angle constrained suboptimal terminal guidance of interceptors for air defence, *In: Proceedings of 18th IFAC Symposium on Automatic Control in Aerospace*, Nara, Japan, 6-10 September 2010, pp.130-135.

[12] Ryoo CK, Cho H and Tahk MJ, Optimal guidance laws with terminal impact angle constraint, *J Guidance Cont Dynam*, Vol.28, No.4, 2005, pp. 724–732.

[13] Ryoo CK, Cho H and Tahk MJ, Time-to-go weighted optimal guidance with impact angle constraints, *IEEE T Contr Syst T*, Vol.14, No.3, 2006, pp. 483–492.

[14] Ratnoo A and Ghose D, Impact angle constrained guidance against nonstationary nonmaneuvering targets, *J Guidance Cont Dynam*, Vol.33, No.1, 2010, pp. 269–275.

[15] Turetsky V and Shinar J, Missile guidance laws based on pursuit-evasion game formulations, *Automatica*, Vol.39, No.4, 2003, pp. 607-618.

[16] Adler FP, Missile guidance by three-dimensional proportional navigation, *J Appl Phys*, Vol.27, No.5, 1956, pp. 500-507.

[17] Xu XY and Cai YL, Optimal guidance law and control of impact angle for the Kinetic Kill Vehicle, *Proc IMechE, Part G, Journal of Aerospace Engineering*, Vol.225, No.9, 2011, pp. 1027~1036.

[18] Ben-Asher JZ and Yaesh I, *Advances in Missile Guidance Theory, vol. 180, Progress in Astronautics and Aeronautics*, AIAA, Reston, VA, 1998, pp. 25–90.

[19] Garber V, Optimum Intercept Laws for Accelerating Targets, *AIAA Journal*, Vol.6, No.11, 1968, pp. 2196–2198.

Appendix

1. proof of Eq.(15)

$\Phi(t_f, t)$ is the transition matrix of the original homogeneous system, and $\Phi(t_f, t)$ can be obtained

though solving equation

$$\dot{\mathbf{x}}(t) = \mathbf{A}\mathbf{x}(t) \tag{A1}$$

The solution of Eq.(A1) is

$$\mathbf{x}(t) = \mathbf{e}^{\mathbf{A}t} = \mathbf{L}^{-1}\{(\mathbf{s}\mathbf{I} - \mathbf{A})^{-1}\}$$

$$= \mathbf{L}^{-1} \begin{bmatrix} s & -1 & 0 & 0 \\ 0 & s & -\cos \gamma_{E0} & 0 \\ 0 & 0 & s + 1/\tau_E & 0 \\ 0 & 0 & -1/V_E & s \end{bmatrix}^{-1}$$

$$= \mathbf{L}^{-1} \begin{bmatrix} \frac{1}{s} & \frac{1}{s^2} & \frac{\cos \gamma_{E0}}{s^2(s + 1/\tau_E)} & 0 \\ 0 & \frac{1}{s} & \frac{\cos \gamma_{E0}}{s(s + 1/\tau_E)} & 0 \\ 0 & 0 & \frac{1}{(s + 1/\tau_E)} & 0 \\ 0 & 0 & \frac{1}{V_E s(s + 1/\tau_E)} & \frac{1}{s} \end{bmatrix}$$

$$= \begin{bmatrix} 1 & t & (-\tau_E^2 + \tau_E t + \tau_E^2 e^{-\frac{t}{\tau_E}}) \cos \gamma_{E0} & 0 \\ 0 & 1 & (\tau_E - \tau_E e^{-\frac{t}{\tau_E}}) \cos \gamma_{E0} & 0 \\ 0 & 0 & e^{-\frac{t}{\tau_E}} & 0 \\ 0 & 0 & \frac{(\tau_E - \tau_E e^{-\frac{t}{\tau_E}})}{V_E} & 1 \end{bmatrix} \tag{A2}$$

Replace t with $t_f - t$, one obtain the transition matrix

$$\Phi(t_f, t) = \mathbf{e}^{\mathbf{A}(t_f-t)}$$

$$= \begin{bmatrix} 1 & t_f - t & (-\tau_E^2 + \tau_E(t_f - t) + \tau_E^2 e^{-\frac{t_f-t}{\tau_E}}) \cos \gamma_{E0} & 0 \\ 0 & 1 & (\tau_E - \tau_E e^{-\frac{t_f-t}{\tau_E}}) \cos \gamma_{E0} & 0 \\ 0 & 0 & e^{-\frac{t_f-t}{\tau_E}} & 0 \\ 0 & 0 & \frac{(\tau_E - \tau_E e^{-\frac{t_f-t}{\tau_E}})}{V_E} & 1 \end{bmatrix} \tag{A3}$$

And

$$\dot{\Phi}(t_f, t) = -\mathbf{e}^{\mathbf{A}(t_f-t)} \mathbf{A} = -\Phi(t_f, t) \mathbf{A} \tag{A4}$$

Then

$$\begin{aligned} \dot{\mathbf{Z}}(t) &= \mathbf{D}\dot{\Phi}(t_f, t)\mathbf{x}(t) + \mathbf{D}\Phi(t_f, t)\dot{\mathbf{x}}(t) \\ &= -\mathbf{D}\Phi(t_f, t)\mathbf{A}\mathbf{x}(t) + \mathbf{D}\Phi(t_f, t)(\mathbf{A}\mathbf{x}(t) + \mathbf{B}\mathbf{u}_p(t) + \mathbf{C}\mathbf{u}_E(t)) \\ &= \mathbf{D}\Phi(t_f, t)\mathbf{B}\mathbf{u}_p(t) + \mathbf{D}\Phi(t_f, t)\mathbf{C}\mathbf{u}_E(t) \end{aligned} \tag{A5}$$

This completes the proof of Eq.(15)

2. Proof of Eqs. (23-32)

According to Eqs.(19) and (22), the Hamiltonian of the problem can be expressed as

$$H = \frac{1}{2}u^2 - \frac{1}{2}\mu^2v^2 + \lambda_1\dot{Z}_1 + \lambda_2\dot{Z}_2 \quad (A6)$$

The adjoint equations can be expressed as

$$\begin{cases} \dot{\lambda}_1 = -\frac{\partial H}{\partial Z_1} = 0 \\ \dot{\lambda}_2 = -\frac{\partial H}{\partial Z_2} = 0 \end{cases} \quad (A7)$$

The solutions of Eq.(A7) are

$$\begin{cases} \lambda_1(t) = \lambda_1(t_f) = a_1Z_1(t_f) \\ \lambda_2(t) = \lambda_2(t_f) = a_2[Z_2(t_f) - \gamma_f] \end{cases} \quad (A8)$$

The optimal guidance laws of the adversaries can be obtained

$$\begin{cases} \frac{\partial H}{\partial u} = 0 \Rightarrow u^*(t) = -\lambda_1(t)\frac{\partial \dot{Z}_1}{\partial u} - \lambda_2(t)\frac{\partial \dot{Z}_2}{\partial u} \\ \frac{\partial H}{\partial v} = 0 \Rightarrow v^*(t) = \frac{1}{\mu^2}(\lambda_1(t)\frac{\partial \dot{Z}_1}{\partial v} + \lambda_2(t)\frac{\partial \dot{Z}_2}{\partial v}) \end{cases} \quad (A9)$$

Substituting Eqs. (22) and (A8) into Eq. (A9), one can obtain the optimal guidance laws of the adversaries

$$\begin{cases} u^*(t) = a_1t_gZ_1(t_f) - \frac{a_2}{V_p}[Z_2(t_f) - \gamma_f] \\ v^*(t) = \frac{1}{\mu^2}[a_1t_gZ_1(t_f) + \frac{a_2}{V_E}(Z_2(t_f) - \gamma_f)] \end{cases} \quad (A10)$$

Substituting Eq. (A10) into Eq. (22), and integrating from t to t_f ,

$$\begin{aligned} -Z_1(t) &= \int_t^{t_f} [(-1 + \frac{1}{\mu^2})a_1Z_1(t_f)(t_f - t)^2 + (\frac{1}{V_p} + \frac{1}{\mu^2V_E})a_2[(Z_2(t_f) - \gamma_f)(t_f - t)]]dt \\ &= -(-1 + \frac{1}{\mu^2})a_1Z_1(t_f)\frac{(t_f - t)^3}{3} \Big|_t^{t_f} - (\frac{1}{V_p} + \frac{1}{\mu^2V_E})a_2(Z_2(t_f) - \gamma_f)\frac{(t_f - t)^2}{2} \Big|_t^{t_f} + c_1 \\ &= (-1 + \frac{1}{\mu^2})a_1Z_1(t_f)\frac{(t_f - t)^3}{3} + (\frac{1}{V_p} + \frac{1}{\mu^2V_E})a_2(Z_2(t_f) - \gamma_f)\frac{(t_f - t)^2}{2} + c_1 \end{aligned} \quad (A11)$$

Where c_1 is a constant, and

$$c_1 = -Z_1(t_f) \quad (A12)$$

Substituting Eq. (A12) into Eq. (A11)

$$\begin{aligned} Z_1(t_f) &= Z_1(t) + (-1 + \frac{1}{\mu^2})a_1Z_1(t_f)\frac{(t_f - t)^3}{3} \\ &\quad + (\frac{1}{V_p} + \frac{1}{\mu^2V_E})a_2(Z_2(t_f) - \gamma_f)\frac{(t_f - t)^2}{2} \\ &= Z_1(t) + (-1 + \frac{1}{\mu^2})a_1Z_1(t_f)\frac{t_g^3}{3} + (\frac{1}{V_p} + \frac{1}{\mu^2V_E})a_2(Z_2(t_f) - \gamma_f)\frac{t_g^2}{2} \end{aligned} \quad (A13)$$

Likewise

$$\begin{aligned} -Z_2(t) &= \int_t^{t_f} [(\frac{1}{V_p} + \frac{1}{\mu^2V_E})a_1Z_1(t_f)(t_f - t) + (-\frac{1}{V_p^2} + \frac{1}{\mu^2V_E^2})a_2(Z_2(t_f) - \gamma_f)]dt \\ &= [(-\frac{1}{V_p} + \frac{1}{\mu^2V_E})a_1Z_1(t_f)\frac{(t_f - t)^2}{2} - (-\frac{1}{V_p^2} + \frac{1}{\mu^2V_E^2})a_2(Z_2(t_f) - \gamma_f)(t_f - t)] \Big|_t^{t_f} + c_2 \end{aligned}$$

$$\begin{aligned} &= (\frac{1}{V_p} + \frac{1}{\mu^2V_E})a_1Z_1(t_f)\frac{(t_f - t)^2}{2} \\ &\quad + (-\frac{1}{V_p^2} + \frac{1}{\mu^2V_E^2})a_2(Z_2(t_f) - \gamma_f)(t_f - t) + c_2 \end{aligned} \quad (A14)$$

Where c_2 is a constant, and

$$c_2 = -Z_2(t_f) \quad (A15)$$

Substituting Eq. (A15) into Eq. (A14)

$$\begin{aligned} Z_2(t_f) &= Z_2(t) + (\frac{1}{V_p} + \frac{1}{\mu^2V_E})a_1Z_1(t_f)\frac{(t_f - t)^2}{2} \\ &\quad + (-\frac{1}{V_p^2} + \frac{1}{\mu^2V_E^2})a_2(Z_2(t_f) - \gamma_f)(t_f - t) \\ &= Z_2(t) + (\frac{1}{V_p} + \frac{1}{\mu^2V_E})a_1Z_1(t_f)\frac{t_g^2}{2} \\ &\quad + (-\frac{1}{V_p^2} + \frac{1}{\mu^2V_E^2})a_2(Z_2(t_f) - \gamma_f)t_g \end{aligned} \quad (A16)$$

From (A13), one can obtain

$$Z_1(t_f) = \frac{Z_1(t) + (\frac{1}{V_p} + \frac{1}{\mu^2V_E})a_2(Z_2(t_f) - \gamma_f)\frac{t_g^2}{2}}{1 - (-1 + \frac{1}{\mu^2})a_1\frac{t_g^3}{3}} \quad (A17)$$

Substituting Eq. (A17) into Eq. (A16)

$$\begin{aligned} Z_2(t_f) &= Z_2(t) + (\frac{1}{V_p} + \frac{1}{\mu^2V_E})a_1\frac{t_g^2}{2} \frac{Z_1(t) + (\frac{1}{V_p} + \frac{1}{\mu^2V_E})a_2(Z_2(t_f) - \gamma_f)\frac{t_g^2}{2}}{1 - (-1 + \frac{1}{\mu^2})a_1\frac{t_g^3}{3}} \\ &\quad + (-\frac{1}{V_p^2} + \frac{1}{\mu^2V_E^2})a_2(Z_2(t_f) - \gamma_f)t_g \\ &= Z_2(t) + \frac{a_1t_g^2}{3\mu^2 - (1 - \mu^2)a_1t_g^2} Z_1(t) \\ &\quad + \frac{(\mu^2V_E' + V_p')^2}{\mu^2V_E'V_p'} \frac{a_1a_2t_g^4}{4} \\ &\quad + [\frac{V_p'^2 - \mu^2V_E'^2}{3\mu^2 - (1 - \mu^2)a_1t_g^2} + \frac{V_p'^2 - \mu^2V_E'^2}{\mu^2V_E'^2V_p'^2} a_2t_g](Z_2(t_f) - \gamma_f) \end{aligned} \quad (A18)$$

Define

$$\begin{aligned} V_1 &= \frac{V_E'\mu^2 + V_p'}{V_p'V_E'\mu^2} \\ V_2 &= \frac{V_p'^2 - \mu^2V_E'^2}{V_p'^2V_E'^2\mu^2} \\ \Delta &= 3\mu^2 - (1 - \mu^2)a_1t_g^3 \end{aligned}$$

Then

$$Z_2(t_f) = Z_2(t) + \frac{3a_1\mu^2t_g^2V_1}{2\Delta} Z_1(t) + [\frac{3a_1a_2\mu^2t_g^4V_1^2}{4\Delta} + V_2a_2t_g](Z_2(t_f) - \gamma_f) \quad (A19)$$

Define

$$W_1(t_g) = 1 - a_2 V_2 t_g - \frac{3 a_1 a_2 \mu^2 V_1^2 t_g^4}{4 \Delta}$$

$$W_2(t_g) = \frac{3 a_1 \mu^2 V_1 t_g^2}{2 \Delta}$$

Then

$$Z_2(t_f) - \gamma_f = \frac{\frac{3 a_1 \mu^2 t_g^2 V_1}{2 \Delta} Z_1(t) + Z_2(t) - \gamma_f}{1 - \left(\frac{3 a_1 a_2 \mu^2 t_g^4 V_1^2}{4 \Delta} + V_2 a_2 t_g \right)} = \frac{W_2(t_g) Z_1(t) + Z_2(t) - \gamma_f}{W_1(t_g)} \tag{A20}$$

Substituting Eq. (A20) into Eq. (A7)

$$Z_1(t_f) = \frac{Z_1(t) + \frac{\mu^2 V_E + V_P}{\mu^2 V_E V_P} \frac{a_2 t_g^2}{2} \frac{W_2(t_g) Z_1(t) + Z_2(t) - \gamma_f}{W_1(t_g)}}{\frac{3 \mu^2 - (1 - \mu^2) a_1 t_g^2}{3 \mu^2}} = \frac{[2 W_1(t_g) + V_1 a_2 t_g^2 W_2(t_g)] Z_1(t) + V_1 a_2 t_g^2 [Z_2(t) - \gamma_f]}{2 \Delta W_1(t_g)} \tag{A21}$$

Substituting Eqs. (A20) and (A21) into Eq. (A10)

$$u^*(t) = a_1 t_g Z_1(t_f) - \frac{a_2}{V_P} [Z_2(t_f) - \gamma_f] = \frac{a_1 t_g [2 W_1(t_g) + V_1 a_2 t_g^2 W_2(t_g)] Z_1(t) + V_1 a_1 a_2 t_g^3 [Z_2(t) - \gamma_f]}{2 \Delta W_1(t_g)} - \frac{a_2 W_2(t_g) Z_1(t) + a_2 (Z_2(t) - \gamma_f)}{V_P W_1(t_g)} = \left[\frac{3 \mu^2 a_1 t_g}{\Delta} + \frac{a_2 W_2(t_g)}{W_1(t_g)} \left(\frac{3 \mu^2 V_1 a_1 t_g^3}{2 \Delta} - \frac{1}{V_P} \right) \right] Z_1(t) + \frac{a_2}{W_1(t_g)} \left(\frac{3 \mu^2 V_1 a_1 t_g^3}{2 \Delta} - \frac{1}{V_P} \right) (Z_2(t) - \gamma_f) \tag{A22}$$

Define

$$A_1 = \frac{3 a_1 \mu^2 t_g^3}{\Delta} + \frac{a_2 W_2(t_g) t_g^2}{W_1(t_g)} \left(\frac{3 a_1 \mu^2 V_1 t_g^3}{2 \Delta} - \frac{1}{V_P} \right)$$

$$A_2 = \frac{a_2 t_g}{V_P W_1(t_g)} \left(\frac{3 a_1 \mu^2 V_1 t_g^3}{2 \Delta} - \frac{1}{V_P} \right)$$

Then

$$u^*(t) = \frac{A_1}{t_g^2} Z_1(t) - \frac{A_2 V_P}{t_g} [Z_2(t) - \gamma_f] \tag{A23}$$

Likewise

$$v^*(t) = \frac{1}{\mu^2} a_1 t_g Z_1(t_f) + \frac{a_2}{\mu^2 V_E} [Z_2(t_f) - \gamma_f]$$

$$= \frac{a_1 t_g [2 W_1(t_g) + V_1 a_2 t_g^2 W_2(t_g)] Z_1(t) + V_1 a_2 t_g^2 [Z_2(t) - \gamma_f]}{\mu^2 \frac{2 \Delta W_1(t_g)}{3 \mu^2}} + \frac{a_2}{\mu^2 V_E} \frac{W_2(t_g) Z_1(t) + (Z_2(t) - \gamma_f)}{W_1(t_g)} = \frac{1}{\mu^2} \left[\frac{3 \mu^2 a_1 t_g}{\Delta} + \frac{a_2 W_2(t_g)}{W_1(t_g)} \left(\frac{3 \mu^2 a_1 V_1 t_g^3}{2 \Delta} + \frac{1}{V_E} \right) \right] Z_1(t) + \frac{a_2}{\mu^2 W_1(t_g)} \left(\frac{3 \mu^2 a_1 V_1 t_g^3}{2 \Delta} + \frac{1}{V_E} \right) (Z_2(t) - \gamma_f) \tag{A24}$$

Define

$$B_1 = \frac{1}{\mu^2} \left[\frac{3 a_1 \mu^2 t_g^3}{\Delta} + \frac{a_2 W_2(t_g) t_g^2}{W_1(t_g)} \left(\frac{3 a_1 \mu^2 V_1 t_g^3}{2 \Delta} + \frac{1}{V_E} \right) \right]$$

$$B_2 = \frac{a_2 t_g}{\mu^2 V_P W_1(t_g)} \left(\frac{3 a_1 \mu^2 V_1 t_g^3}{2 \Delta} + \frac{1}{V_E} \right)$$

Then

$$v^*(t) = \frac{B_1}{t_g^2} Z_1(t) - \frac{B_2 V_P}{t_g} [Z_2(t) - \gamma_f] \tag{A25}$$

This completes the proof of Eq.(23-32).